Postprint of: Wójcik N. A., Jonson B., Möncke D., Kamitsos E. I., Segawa H., Karczewski J., Ali S., The effect of nitrogen on the structure and thermal properties of beryllium-containing Na-(Li)-Si-O-N glasses, Journal of Non-Crystalline Solids, Vol. 522, (2019), 119585, DOI: 10.1016/j.jnoncrysol.2019.119585

The effect of nitrogen on the structure and thermal properties of beryllium-containing Na-(Li)-Si-O-N glasses

N. A. Wójcik[1,2*], B. Jonson[2], D. Möncke[2,3,4], E. I. Kamitsos[3], H. Segawa[2,5], J. Karczewski[1], S. Ali[2]

[1] *Department of Solid State Physics, Faculty of Applied Physics and Mathematics, Gdańsk University of Technology, Narutowicza Street 11/12, 80–233 Gdańsk, Poland*

[2] *Department of Built Environment and Energy Technology, Linnaeus University, 35195 Växjö, Sweden*

[3] *Theoretical and Physical Chemistry Institute, National Hellenic Research Foundation, 48 Vassileos Constantinou Avenue, 11635 Athens, Greece*

[4] *Inamoris School of Engineering at the New York State College of Ceramics, Alfred University, 1 Saxon Drive, 14802 Alfred, NY, USA*

[5] *National Institute for Materials Science, 1-1 Namiki, Tsukuba 305-0044, Japan*

**corresponding author:* natalia.wojcik@pg.edu.pl, natalia.wojcik@lnu.se

Keywords: Oxynitride glasses, Beryllium-silicate glasses, Raman spectroscopy, Thermal properties

Abstract

Two oxynitride glass series with the composition of $35Na_2O$-5BeO-(60-x)SiO_2-xSi_3N_4 and $9Li_2O$-$27Na_2O$-5BeO-(59-x)SiO_2-xSi_3N_4, were prepared. The glasses' topography and structure were studied by Scanning Electron Microscopy and Raman spectroscopy. The composition was analyzed by Inductively Coupled Plasma Optical Emission Spectrometer, SEM-EDS and nitrogen and oxygen elemental analyzer. Na-(Li)-Be-silicate glasses were found to contain up to approximately 3.4 (or 5.2 for EDS measurements) at% of N, respectively. The samples were homogenous in their topography and compositions of their cross-sections.

The presence of three-fold coordinated nitrogen atoms in Na-Be-Si-O-N glasses results in higher degree of polymerization as was observed by Raman spectroscopy. The spectrum of analogous glasses with lithium did not show a significant decrease in Q^2 units but exhibit the presence of Q^4 units which also indicates a polymerization of the network. The incorporation of nitrogen in these glasses leads to the increase of the glass transition temperature and thermal stability.

1. Introduction

Adding beryllium to silicate glasses opens a very interesting field of research, considering the unique chemical properties of Be^{2+} such as the fact that it has the highest field strength (defined as the charge-to-radius ratio) and the highest

electronegativity among all alkaline-earth and alkali ions. As a consequence, beryllium ions exhibit an electronic polarizability ($\alpha_{Be^{2+}}$ =0.008 Å^3) which is even lower than that characteristic of network-forming cations such as Si^{4+} ($\alpha_{Si^{4+}}$ =0.033 Å^3) [1]. Be^{2+} is always found to be fourfold coordinated to oxygen in crystalline oxides and to form regular, charged $[BeO_4]^{2-}$ tetrahedra [2]. Similarly to Al_2O_3, that can act as network modifier when Al^{3+} ions are octahedrally coordinated or as network former, as charged $[AlO_4]^-$ tetrahedra in the presence of other modifiers [3], the role of BeO in a glass network is both as intermediate glass former which is apparent from the high T_g of beryllium-containing glasses [4], and as a glass-modifier [5] when, for example, considering the silicate Q-unit distribution as monitored by vibrational spectroscopy [6-8].

So far, only few reports exist on the study of the structure and properties of beryllium-containing glasses [9-14]. In our previous work on beryllium containing silicate oxide glasses [5] we have discussed structural variations, as probed by IR and Raman spectroscopy, for BeO substitution of SiO_2 in $35M_2O$-xBeO-(65-x)SiO_2 glasses. Based on our previous findings [5], we see that beryllium forms charged $[BeO_{4/2}]^{2-}$ tetrahedra in the silicate network. The strong cross-linking capacity of these units is shown by a significant increase of the glass transition temperature for the glass series $35M_2O$-xBeO-(65-x)SiO_2 up to 70 ^oC for M_2O=Na_2O; and 44 ^oC for the corresponding mixed Na-Li-glasses. At the same time, the thermal stability decreases (by 107 ^oC for Na-glasses and 155 ^oC for Na-Li-glasses) as BeO substitutes for SiO_2 up to 15 mol% BeO. However, as we showed in ref. [5], vibrational spectroscopy suggests the formation of Si-O-Be bonds though these bonds appear mostly as of non-bridging oxygen atoms on silicate tetrahedra.

Expanding on our previous work, which focused on the role of Be^{2+} ions in glass formation, fundamental scientific questions remain; for example, when considering the low viscosity of Be-silicate melts [15] which is in contrast with the high T_g observed in the system we studied in ref. [5], thus justifying the ongoing research on this glass system. In the current work, we focus on the effect of N incorporation on the structure and thermal properties of Be-containing silicate glasses; this adds data on the lightest alkaline earth cation to the previous studies published on oxynitride alkaline earth silicate glasses [16-22]. While such glasses constitute a significant group of oxy-nitride containing systems [16, 23-27], there is no report yet on the Be-Si-O-N glass system.

Thus, choosing the Be-Silicate glasses for nitridation studies will contribute significantly to our understanding of glass formation and structure, and complement studies on Mg, Ca, Sr and Ba-containing oxy-nitride silicate glasses.

Generally, nitrogen incorporation leads to significant improvements of a number of glass properties such as an increase in glass transition temperature and glass stability [28]; a higher electrical conductivity [29-31] and dielectric constant; higher refractive index; as well as higher elastic modulus and hardness [22, 32]. Most of these changes are due to the fact that nitrogen chemically bonds to silicon or other network forming elements in the glass network. Nitrogen when substituting for oxygen forms 2 and/or 3 bonds instead of the two bonds of a bridging oxygen [30, 31], and this leads to a more covalent and stiffer network. The preparation of oxynitride glasses is much more complex than for the equivalent non-nitrogen glasses as nitridation processes require high melting temperatures, a reducing atmosphere to prevent the oxidation of the melt and crucibles suitable for this process [32]. Moreover, even if these requirements are fulfilled, nitrogen incorporation into the glass network is not always successful and the obtained nitrogen content can be lower than the target one.

The aim of the present work is to elucidate the effects of nitrogen incorporation on the structure and the thermal properties of beryllium-silicate glasses containing single and mixed alkali ions. For this purpose, two different glass series with a composition close to $35M_2O$-5BeO-$(65-x)SiO_2$-xSi_3N_4 were prepared. The first glass series has a high content of Na_2O (35 mol%), while in the second series 9 mol% of Na_2O were substituted by Li_2O. The glasses of our previous study [5] were found to contain also a significant content of Al, which is known to have an analogous effect on the structure and thermal properties of the alkali silicate network as has BeO [6-8]. Aluminum-free glasses are compared with Al-containing glasses of the previous study [5], in consideration of the similar roles of Al and Be as intermediate glass formers. This aspect of the current study is of key importance as many industrial melts are prepared in alumina-containing refractory material and Al_2O_3 dissolution will alter the composition, structure and, consequently, the glass properties as shown before for various glass systems [33-35]. The preparation, structure and thermal properties of new beryllium containing oxynitride silicate glasses are reported here for the first time.

2. Experimental

2.1. Glass preparation

Two series of beryllium-silicate oxynitride glasses containing alkali ions were prepared. The first system of glasses has a composition of $35Na_2O$-5BeO-$(60-x)SiO_2$-xSi_3N_4 and the second one of $9Li_2O$-$27Na_2O$-5BeO-$(59-x)SiO_2$-xSi_3N_4 in mol%, where x increases from 1 to 5 mol%. The glasses were prepared from mixtures of Si_3N_4 (ChemPur GmbH), BeO (99% Alfa Aesar), SiO_2 (99.99% ChemPur GmbH), Na_2CO_3 (99.9+% ChemPur GmbH) and Li_2CO_3 (99.999% ALDRICH). Batches of about 1.3 grams of each composition were placed in niobium crucibles (10 mm diameter). Synthesis was performed under nitrogen atmosphere. The mixtures were melted at 1400–1650 °C, depending on the composition, using a radio frequency furnace [16]. The melting time was about 1 hour. The melts were cooled by turning off the furnace at the end of the run (the approximately cooling time to room temperature was 1 h). During heating, a strong exothermic reaction was observed, and some samples needed to be re-melted in order to obtain a homogenous material. The temperature at which a melt formed was found to increase with increasing amount of Si_3N_4 [16].

Table 1 lists the nominal compositions and the IDs of the synthesized samples. For comparison, Raman spectra and thermal properties from ref. [5] for the four glasses $35Na_2O$–$65SiO_2$, $9Li_2O$–$27Na_2O$–$64SiO_2$, $35Na_2O$-5BeO-$60SiO_2$ and $9Li_2O$-$27Na_2O$-5BeO-$59SiO_2$ (in mol%) were included in this study.

2.2. Glass characterization

2.2.1. Chemical analysis

The chemical composition (lithium, sodium, beryllium and silicon contents) of the samples was investigated using an inductively coupled plasma optical emission spectrometer (ICP-OES, Hitachi High-Technologies Corp., Model SPS3520UV-DD). Measurements were performed after dissolution of the glass powders in a mixture of 2 ml of H_2O, 0.5 ml of HF acid and 5 ml of HNO_3 acid heated at 105 °C. All ICP-OES values are listed in Table 1. The error margins of ICP-OES analysis were +/- 1 % for all elements. Standard substances for ICP measurements were purchased from Kanto Chemical Co., Inc.

Nitrogen and oxygen contents were determined by inert gas fusion technique using a nitrogen and oxygen elemental analyzer (LECO Corp., TC-436AR). Nitrogen

contents were estimated from the thermal conductivity of the N_2 gas and oxygen contents from infrared absorption of CO_2 gas after combustion with He gas. The obtained data for O and N contents has an error exceeding 10 %. In Table 1, the oxygen content under ICP-OES results was determined from the charge requirements of the analyzed cations.

2.2.2. CSLM observations

The topography of the samples was observed using an Olympus LEXT OLS4000 Confocal Scanning Laser Microscope (CSLM). Color imaging was conducted under white LED light, and 3D images were obtained using a 405 nm laser and Photomultiplier Detector. The highest objective lens and laser 3D image magnification used was 100x, with optical magnification of 2160x. CSLM measurements were conducted on alcohol-cleaned samples surfaces.

2.2.3. SEM with EDS

The topography and composition of the samples were additionally investigated using a scanning electron microscope (SEM), FEI Company Quanta FEG250 with Energy Dispersive X-ray Spectrometer (EDAX GENESIS Apex Apollo X60). Measurements were conducted using a 10 kV beam accelerating voltage with a SE-ETD detector (secondary electron—Everhart-Thornley detector) working in the high vacuum mode (pressure 10^{-4} Pa). EDS analysis was carried out for three areas for each sample (for exemplar areas see Fig. 2). It was not possible to detect the light elements Be and Li with this technique. Therefore, we used the target values for Be and Li contents and the mean values of EDS results obtained for the other elements, especially Si and Na, to calculate the approximate compositions of all samples assuming no significant loss of Li and Be during melting. All EDS values are given with an accuracy of around ± 5% standard deviation. The results are displayed in Table 1 as EDS analyzed glass compositions. The sensitivity of our SEM-EDS equipment allows to detect nitrogen only in those samples in which the N content was higher than 3 at%. The other samples contain N level below 3 at% (marked in Table1 as $N_{<3}$).

2.2.4. Raman spectroscopy

Raman spectra were obtained in the range from 100 to 2000 cm^{-1} with a resolution of 2 cm^{-1} with a dispersive confocal Raman microscope (Renishaw inVia) using the 514.5 and 633 nm laser excitation lines. The sample spot size of the Raman microscope is about 0.5 µm in diameter. Spectra have been normalized to the intensity of the high frequency envelop at about 1090 cm^{-1}, to allow for better comparison. Some spectra were distorted by underlying fluorescence. Here, baseline subtraction was employed.

2.2.5. DTA analysis

The thermal properties of the glasses were investigated by differential thermal analysis (DTA). DTA measurements were performed up to 1100 °C on powdered samples placed in Al_2O_3 crucibles, under flowing nitrogen with a NETZSCH STA 409PC instrument and a heating rate of 20 °$Cmin^{-1}$. The onset of an endothermic drift found on the DTA curve were taken as representing T_g. The exothermic processes observed in all samples are correlated with various crystallization processes. The thermal properties parameters were estimated with the use of dedicated software. The precision in the determination of thermal processes depends on the selected temperature range and varies up to ± 2 % of the determined value.

3. Results and discussion

3.1. Chemical composition and topography measurements

Ten beryllium-silicate oxynitride glasses containing either sodium and/or lithium ions were prepared in radio frequency furnace. Melting under nitrogen atmosphere with addition of Si_3N_4 resulted in dark-grayish, shiny and translucent glass samples. The samples become less shiny and translucent with an increase in Si_3N_4. This change in color is expected since oxynitride glasses are normally less transparent than the equivalent oxide glasses. They usually present a greyish-black color and are only translucent in thin sections [32].

The target and analyzed compositions of the (Li)-Na-Be-Si-O-(N) glass series are listed in Table 1. Samples IDs are based on the nominal xSi_3N_4 quantity in mol% (x = 1, 2, 3, 4 or 5) and suggest glass series with sodium (xNNaBe) or sodium and lithium

(xNLiNaBe). The compositions were evaluated with three techniques. The nitrogen content was estimated with the nitrogen analyzer, which is more sensitive for nitrogen detection than the EDS technique. However, as mentioned earlier, the N results should be taken as approximate values only, since we could not get all samples measured with the necessary extraction time for high accuracy. However, N-analysis by gas analyzer was able to measure low nitrogen levels that increase from 0.9 for glasses doped with 1 mol% of Si_3N_4) to ~3.4 at% for glasses doped with 5 mol% of Si_3N_4. ICP-OES was employed in order to directly measure the light elements lithium and beryllium which are not detectable by SEM-EDS. All cations (Na, Li, Be and Si) were found in the glasses in similar levels as expected from the target compositions.

SEM-EDS was initially used to confirm the elemental analysis, including Al-impurities from the crucible. Since the elements Li and Be are too light to be detected by SEM-EDS, their levels were assumed to equal the nominal compositions and the presented data added Li and Be levels relative to the analyzed Si content. It is worth to note that only three samples with lithium addition (3NLiNaBe, 4NLiNaBe and 5NLiNaBe) contain a nitrogen level that could be detected by SEM-EDS (> 3 at%).

Overall, the analyzed compositions contain slightly less Si than the target glasses. The difference is especially obvious for glasses with detectable N content (glasses 3NLiNaBe, 4NLiNaBe and 5NLiNaBe). One explanation could be the formation of the reduced volatile SiO species during the melting process. For most of glasses, the N content estimated by SEM-EDS and nitrogen analyzer (ICP-OES in Table 1) are in good agreement, although the N contents estimated by EDS measurements in three samples, 3NLiNaBe, 4NLiNaBe and 5NLiNaBe, are slightly higher than those by the nitrogen analyzer. Since SEM-EDS measurements were done only for three selected areas, and contents of Li and Be elements could not be determined at all, we decided to base our discussion on ICP-OES and nitrogen analyzer results.

The fact that the estimated N content is generally lower than the nominal (aimed) N content can be explained by the presence of CO_2 (carbonate) in the raw materials, which during release acts against N incorporation into the glass network [24]. This is due to CO_2 from carbonates which may oxidize Si_3N_4 according to the reactions:

$$MCO_3 \rightarrow MO + CO_2 \quad (1)$$

$$Si_3N_4 + 6CO_2 \rightarrow 3SiO_2 + 6CO\,(g) + 2N_2\,(g) \quad (2)$$

leading to N_2 loss. Also, Si_3N_4 can decompose in batch according to:

$$Si_3N_4(s) \rightarrow 3Si\ (l) + 2N_2\ (g) \qquad (3)$$

leading to frothing in O–N glass melt [24]. In this case, N incorporation into the glass structure is depressed. Moreover, the vapor pressure of decomposition for Si_3N_4 releasing N_2 can rise above atmospheric pressure at temperatures as low as 1400°C [36, 37].

Table 1 Glasses IDs, target and analyzed EDS and ICP-OES compositions in at%. For comparison, data are included for glasses $35M_2O$-$65SiO_2$ and $5BeO–35M_2O–60SiO_2$ taken from ref.[5].

Sample ID	Target composition (in at%)	SEM-EDS (in at%)	ICP-OES (in at%)
		$35Na_2O$-5BeO-$(60-x)SiO_2$-xSi_3N_4	
1NNaBe	$Na_{24.4}Be_{1.7}Si_{20.2}O_{52.3}N_{1.4}$	$Na_{22.3}Be_{1.7}Si_{21}O_{54.9}N_{<3}$	$Na_{23.6}Be_{1.8}Si_{21.4}O_{52.3}N_{0.9}$
2NNaBe	$Na_{23.1}Be_{1.7}Si_{21.1}O_{51.5}N_{2.6}$	$Na_{26.8}Be_{1.5}Si_{18.9}O_{52.8}N_{<3}$	$Na_{23.2}Be_{1.8}Si_{22}O_{51.5}N_{1.4}$
3NNaBe	$Na_{22.8}Be_{1.6}Si_{21.5}O_{50.2}N_{3.9}$	$Na_{26.2}Be_{1.5}Si_{19.3}O_{53.1}N_{<3}$	$Na_{23.1}Be_{1.7}Si_{22.8}O_{50.2}N_{2.1}$
4NNaBe	$Na_{22.5}Be_{1.6}Si_{21.9}O_{48.9}N_{5.1}$	$Na_{24}Be_{1.5}Si_{20.3}O_{54.2}N_{<3}$	$Na_{23.5}Be_{1.8}Si_{22.8}O_{48.9}N_3$
5NNaBe	$Na_{22.2}Be_{1.6}Si_{22.2}O_{47.6}N_{6.3}$	$Na_{22.2}Be_{1.5}Si_{21.2}O_{55}N_{<3}$	$Na_{23.8}Be_{1.8}Si_{23.6}O_{47.6}N_{3.2}$
		$9Li_2O$-$27Na_2O$-5BeO-$(59-x)SiO_2$-xSi_3N_4	
1NLiNaBe	$Li_6Na_{18.1}Be_{1.7}Si_{20.4}O_{52.5}N_{1.3}$	$Li_{5.8}Na_{19.2}Be_{1.6}Si_{19.7}O_{53.6}N_{<3}$	$Li_{6.8}Na_{16.8}Be_{1.8}Si_{21.2}O_{52.5}N_{0.9}$
2NLiNaBe	$Li_{5.9}Na_{17.8}Be_{1.7}Si_{20.8}O_{51.2}N_{2.6}$	$Li_{5.5}Na_{20.5}Be_{1.5}Si_{19.3}O_{53.1}N_{<3}$	$Li_{6.9}Na_{16.9}Be_{1.8}Si_{21.6}O_{51.2}N_{1.5}$
3NLiNaBe	$Li_{5.9}Na_{17.6}Be_{1.6}Si_{21.2}O_{49.8}N_{3.9}$	$Li_{5.2}Na_{19.9}Be_{1.4}Si_{18.6}O_{53.1}N_{3.6}$	$Li_{6.9}Na_{17.5}Be_{1.8}Si_{21.8}O_{49.8}N_2$
4NLiNaBe	$Li_{5.8}Na_{17.4}Be_{1.6}Si_{21.5}O_{48.6}N_{5.1}$	$Li_{4.7}Na_{21.8}Be_{1.3}Si_{17.5}O_{49.5}N_{5.2}$	$Li_7Na_{17.6}Be_{1.8}Si_{22.1}O_{48.6}N_{2.9}$
5NLiNaBe	$Li_{5.7}Na_{17.1}Be_{1.6}Si_{21.9}O_{47.3}N_{6.3}$	$Li_{4.8}Na_{19.6}Be_{1.3}Si_{18.6}O_{50.7}N_5$	$Li_{7.1}Na_{17.9}Be_{1.9}Si_{22.5}O_{47.3}N_{3.4}$
		$35M_2O$-$65SiO_2$ and $35M_2O$–5BeO–$60SiO_2$ [5]	
0Na	$Na_{23.3}Si_{21.7}O_{55}$	$Na_{19.2}Al_{0.5}Si_{23.3}O_{57}$	$Na_{22.4}Si_{21.1}Al_{0.5}O_{56}$
0NaBe	$Na_{23.7}Be_{1.7}Si_{20.3}O_{54.2}$	$Na_{15.5}Be_{1.9}Al_{1.1}Si_{23.3}O_{58.1}$	$Be_{1.8}Na_{20.7}Si_{20.6}Al_{0.8}O_{56.2}$
0LiNa	$Li_6Na_{18}Si_{21.3}O_{54.7}$	$Li_{5.8}Na_{18.4}Al_{0.5}Si_{20.8}O_{54.5}$	$Li_{6.7}Na_{17}Si_{21.3}Al_{0.4}O_{54.6}$
0NaBeLi	$Li_{6.1}Na_{18.3}Be_{1.7}Si_{20}O_{53.9}$	$Li_6\ Na_{14.7}Be_{1.8}Al_{2.5}Si_{19.8}O_{55.3}$	$Li_8\ Na_{16.6}Be_{1.7}Si_{17}Al_{2.8}O_{53.9}$

Figure 1(a) presents the CSLM image for glass 4NNaBe. Its topography looks like a typical glass surface [38]. The other glasses of the xNNaBe series show a similar glossy topography with grayish color. The topography of glass 1NLiNaBe is shown in Fig. 1(b). Contrary to the samples of the xNNaBe series, it has a less smooth surface and contains inhomogeneities. The most significant change is observed for the topography of glasses 4NLiNaBe and 5NLiNaBe (Fig. 1(c)). The color of their surfaces is darker, and their topography contains even more inhomogeneities.

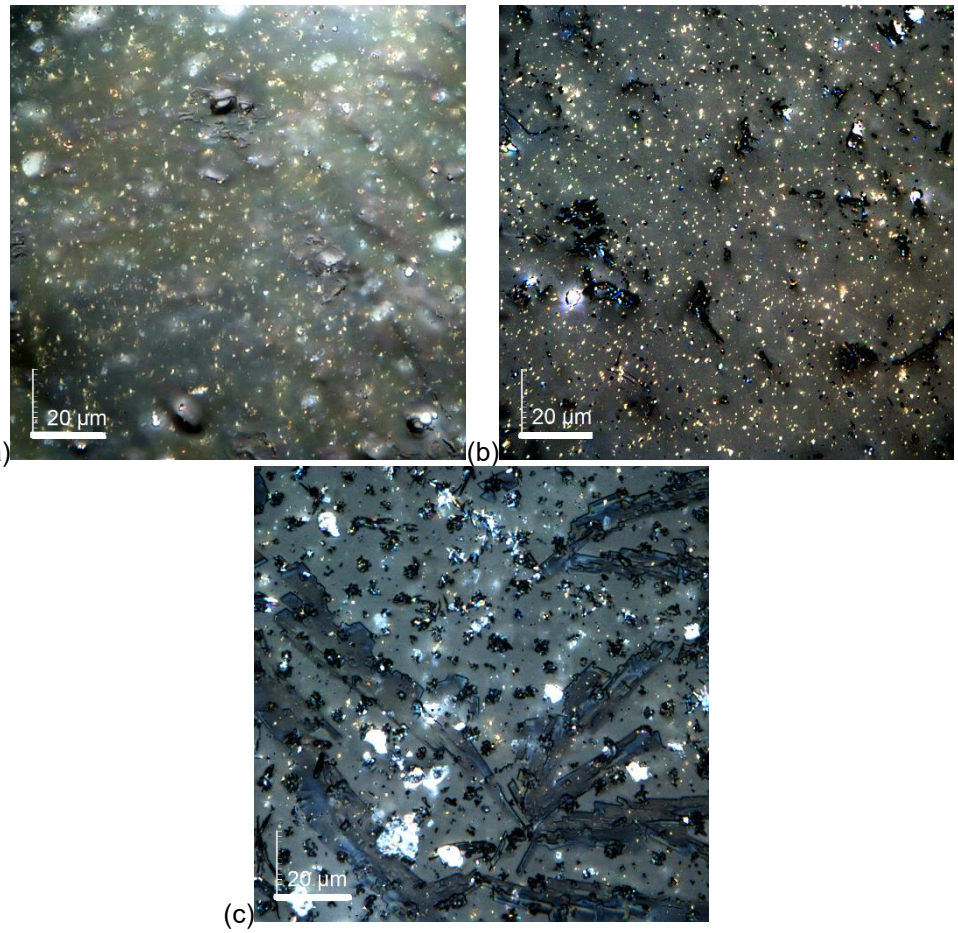

(a) (b) (c)

Figure 1 CSLM micrographs of glasses surfaces: (a) 4NNaBe, (b) 1NLiNaBe and (c) 5NLiNaBe.

SEM micrographs of fresh cross-sections of the glasses 3NNaBe and 4NLiNaBe are presented in Fig. 2 (a) and (b), respectively. Additionally, Fig. 2 (c) depicts the topography of glass 1NNaBe using a higher magnification. The topography of the presented samples is characteristic for homogenous glasses, without any evidence for phase separation or precipitates. Similar micrographs were obtained for all other glasses discussed in this study.

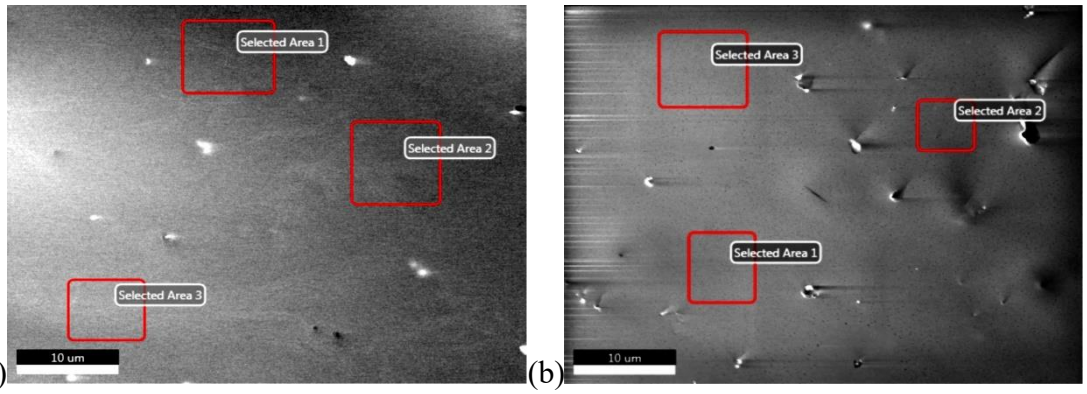

(a) (b)

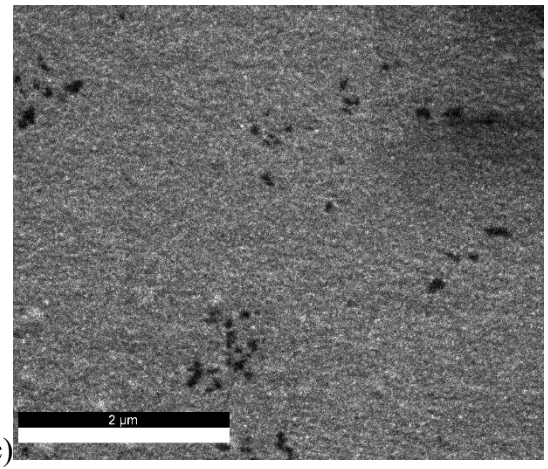

(c)

Figure 2 SEM micrographs for fractured glasses: (a) 3NNaBe, (b) 4NLiNaBe and (c) 1NNaBe (with higher magnification).

3.2. Vibrational spectroscopy

3.2.1. Raman spectra of glasses

Raman spectra of representative samples are shown in Figs 3 and 4. For better understanding of the Raman results we include spectra from reference [5] for the N-free and Be-free glasses $65SiO_2$–$35Na_2O$ and $64SiO_2$–$27Na_2O$–$9Li_2O$ denoted as 0Na and 0LiNa in the following discussion, as well as for the N-free beryllate glasses 5BeO-$60SiO_2$-$35Na_2O$ and 5BeO-$59SiO_2$-$27Na_2O$-$9Li_2O$ denoted as 0NaBe and 0NaBeLi. It should be noted that the last two samples contain traces of Al from dissolution of the crucible material (see Table 1), while Al inclusion is absent from N-containing glasses prepared in Nb crucibles.

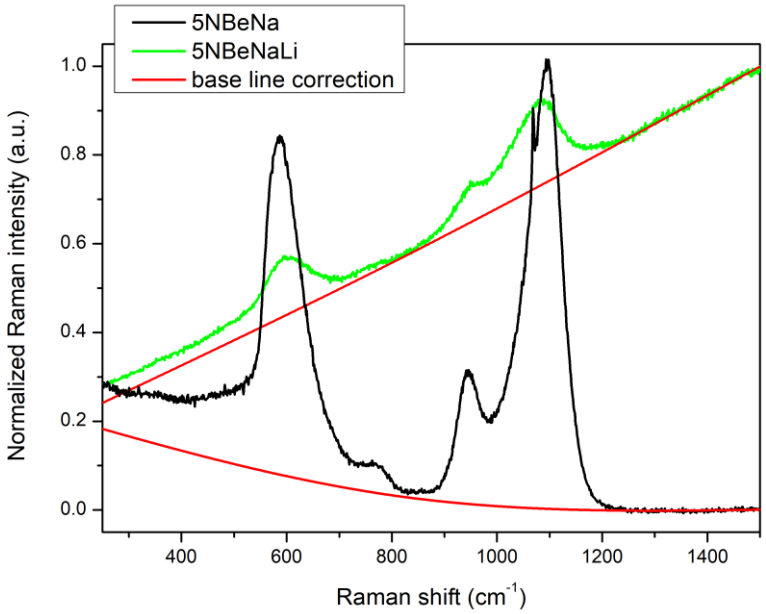

283

284 **Figure 3** Raman spectra for exemplar glasses 5NNaBe and 5NLiNaBe, measured using the 633 and
285 514.5 nm laser excitation lines, respectively. These spectra are not baseline corrected, but adjusted in
286 their intensities for better comparison (red lines give examples for base line subtraction to account for
287 the broad fluorescence bands).

288

289 As seen in Figure 3, significant fluorescence background was found in the Raman
290 spectra of the xN(Li)NaBe series after nitridation. Therefore, background correction
291 needed to be conducted for the baseline above 350 cm^{-1}, and the baseline corrected
292 spectra are shown in Figure 4. We note that some spectra exhibited less fluorescence
293 with 633 nm instead of 514.5 nm excitation. The use of the 488 nm excitation line
294 available to us gave similar fluorescence as the 514.5 nm line. Another option available
295 to us was the 785 nm line, but in silicates this line often gives strong artefacts arising
296 from Nd impurities which results in a strong fluorescing signal [39].

297

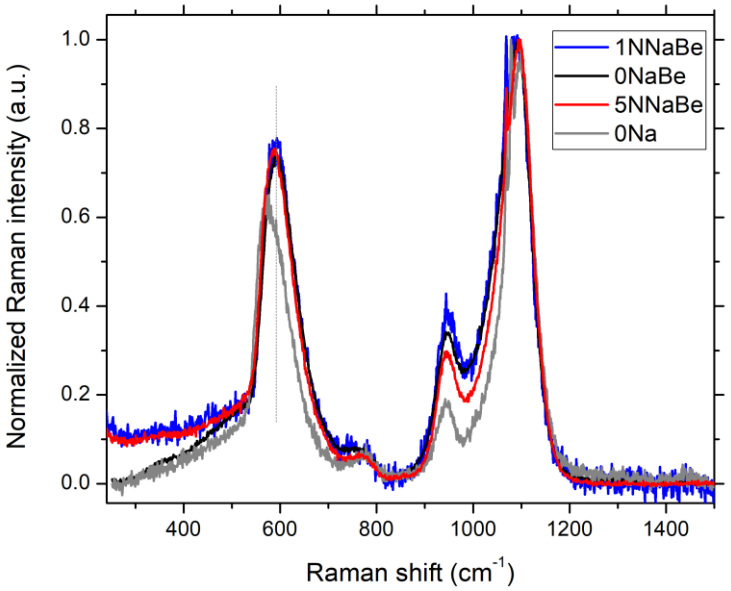

(a)

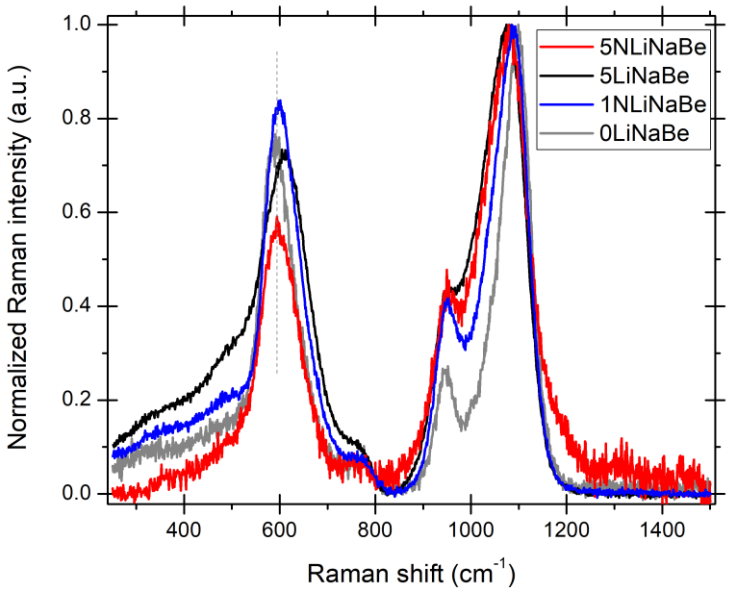

(b)

Figure 4 Raman spectra of glasses in the series **(a)** xNNaBe and **(b)** xNLiNaBe (for glass compositions see Table 1), measured using the 633 and 514.5 nm laser excitation lines, respectively. For comparison, are included the Raman spectra for glasses $35Na_2O$-$65SiO_2$ (0Na) and $35M_2O$–5BeO–$60SiO_2$ (0NaBe and 0LiNaBe) of ref.[5]. All spectra are baseline corrected and normalized to the intensity of the high frequency envelop at about 1090 cm^{-1}.

Exemplar Raman spectra taken from fresh cross-sections of glasses 1N(Li)NaBe and 5N(Li)NaBe are presented in Fig. 4a and b, respectively, for glasses from the

xNNaBe and xNLiNaBe glass series. The plots also include the Raman spectra of the N-free glasses 0(Li)Na and 0(Li)NaBe. The spectra of the nitrogen containing glasses 2N(Li)NaBe to 4N(Li)NaBe overlay pretty much the spectra of glasses 1N(Li)NaBe, especially when considering the uncertainties of fluorescence and base line correction and are therefore not included in Fig.4.

All Raman spectra show a very strong band at ~1090 cm^{-1}, which is typical for a high connected silicate network as this band is due to the symmetric stretching mode of Si-O bonds in Q^3 units, ν(Si-O) Q^3 [3, 40-42]. In addition, all spectra show a pronounced contribution on the low-energy side of the 1090 cm^{-1} band, reflecting the presence of Q^2 groups (ca. 950 cm^{-1}). The weak Raman feature at ~770 cm^{-1} is assigned to the symmetric bending vibration of Si-O-Si bridges, while the intense Raman band at ~590 cm^{-1} reflects a combination of stretching and bending modes of the Si-O-Si bridges [3, 40-42]. This last band depends strongly on the connectivity of the silicate network, and for a glass structure dominated by Q^3 tetrahedra its position is observed close to 570 cm^{-1} [40, 41].

For both the Raman spectra of the studied series in Fig.4a and 4b, with and without lithium addition, we observe the highest Q^3 and lowest Q^2 relative intensities for the alkali-silicate glasses without beryllium or nitrogen additions (0Na and 0LiNa). As discussed in detail in our previous work [5], BeO and Al_2O_3 substitution for SiO_2 (as in 0NaBe(Li)), will increase the signature of Q^2 bands as Be-O-Si and Al-O-Si bridges form between $SiO_{4/2}$ and $[BeO_{4/2}]^{2-}$ or $[AlO_{4/2}]^{-}$ tetrahedra; both of the latter are charge balanced by Na^+ and/or Li^+ ions from modifier oxides that are in turn not available for the depolymerization of the silicate network.

In the sodium series, the sodium levels are slightly higher in the nitride-containing xNLiNaBe glasses than the N-free samples, while the silicate content is slightly lower and the BeO level is lower than the BeO and Al_2O_3 levels in the glass 0NaBe. Contrary to a higher alkali content, which would increase the Q^2 fraction, a lower BeO (and Al_2O_3) level will decrease the Q^2 content and increase the Q^3 fraction. Compared to the 0NaBeLi glass, the composition of the nitrided xNLiNaBe glasses is higher in the silicate content and slightly lower in Li_2O content, while the content of BeO is lower than the BeO and Al_2O_3 level in the glass 0NaBeLi. Therefore, similar changes for Raman spectra should be observed as for glasses without lithium. From Figure 4, it is apparent that both effects are of similar magnitude.

3.2.2. Effect of nitrogen addition on Raman spectra

In both the xN(Li)NaBe series, the Raman spectrum of the glass with x=5 shows a higher Q^3:Q^2 ratio than for x=1, though glasses with x=2 to 4 are closer to x=1 in appearance. No steady evolution is seen with nitrogen addition, even when comparing the spectra of the three glasses 3-5NLiNaBe for which a significant nitrogen content could be confirmed by SEM-EDS. The decrease in the Q^2 band for sample 5NNaBe is indicative for a higher network polymerization caused by the presence of three-fold coordinated nitrogen atoms in silicate glasses. Of interest is the spectrum of glass 5NLiNaBe (Fig. 4b) which, even though it does not show a significant decrease in Q^2 units, shows a shoulder at about 1190 cm^{-1} which is indicative of Q^4 units. This feature signals the polymerization of the network for the sample with the highest nitrogen addition. The band position of the mixed symmetric stretching-bending modes of Si-O-Si at about 590 cm^{-1} is slightly higher for glasses 0(Li)NaBe and 1N(Li)NaBe which are both more depolymerized, than glasses 0(Li)Na and 5N(Li)NaBe. As discussed before, the type of polymerization in glasses 0(Li)Na and 5N(Li)NaBe is quite different. Glasses 0(Li)Na have more Si-O-Si bridges, glass 5N(Li)NaBe more Si-N-Si bridges and Si-O-Be bridges, the oxygen of the latter appearing as non-bridging in the Raman spectra (Q^2, Q^3 units). It should be noted here that Si_3N_4 addition will increase the degree of network polymerization regardless of subsequent N⇔O exchange, as more network former elements (Si) are added to a constant reservoir of network modifiers.

3.2.3. Raman spectra of the small fraction heterogeneities

While measuring the spectra of N-containing glasses, by focusing the Raman microscope on vitreous areas of the samples, we noticed the presence of some crystalline inclusions and impurities from the niobium crucibles. As an example, Figure 5a shows the Raman spectra of such heterogeneous sample spots, where several spectra show sharp bands at 1077 cm^{-1} and 520 cm^{-1}. These bands can be attributed to crystalline silicates such as $Na_2Si_2O_5$ [43] or $Na_6Si_8O_{19}$ [44], while a sharp signal at 540 cm^{-1} in xNLiNaBe glasses (not shown in Fig.5a) indicates the formation of crystalline $Li_2Si_2O_5$ [45].

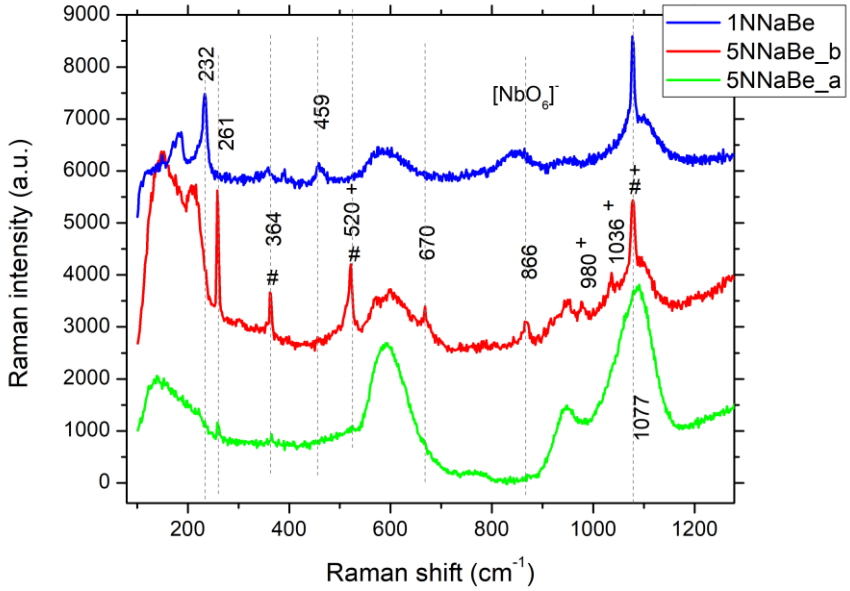

(a)

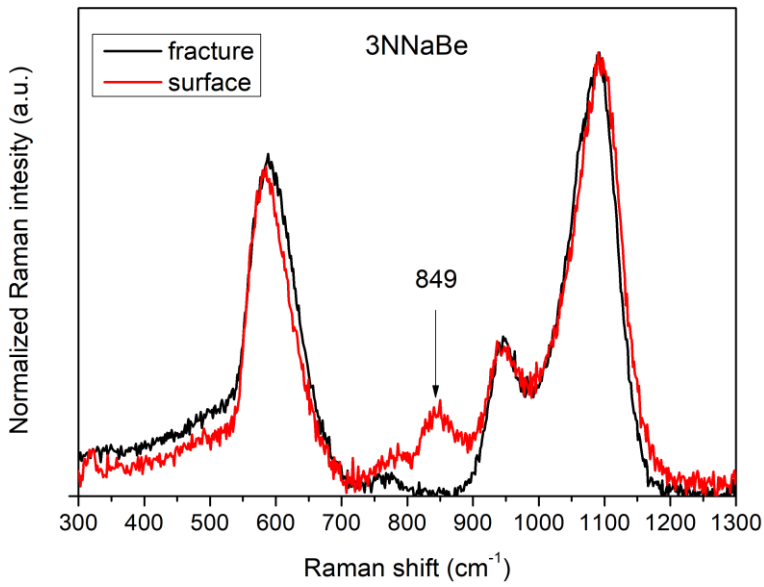

(b)

Figure 5 (a) Raman spectra of heterogeneous spots for glasses 1NNaBe and 5NNaBe and (b) Raman spectra of glass 3NNaBe measured on a fresh cross-section (black) and the surface (red) which was in contact with the Nb crucible. Sharp bands in (a) marked with # and + indicate the formation of crystalline $Na_6Si_8O_{19}$ (Q^3:Q^4=3:1) and α-$Na_2Si_2O_5$, respectively. Spectra were measured using the 633 nm laser excitation line.

The comparison of Raman measurements conducted on the cross-section and surface of glass 3NNaBe is displayed in Fig. 5b. The Raman spectrum of the glass

surface exhibits an additional band at ~849 cm^{-1} which can be assigned to highly distorted NbO_6 octahedra [45]. The high polarizability of Nb ions compared to the polarizability of silicate cations, results in an exceptional high scattering cross section for Nb-O related bands and, thus, traces of dissolved Nb-impurities can be identified by Raman spectroscopy. It is of interest to note that we could reproducibly identify Nb-related bands when measuring on the original sample surface which was in contact with the Nb-crucible. However, the Nb-signature band at 849 cm^{-1} is absent from the spectra taken from within the bulk of glasses by focusing on the inside of broken off glass pieces. Thus, the presence of Nb in the glass surface in contact with the crucible is a consequence of the synthesis route employed. Contrary to a previous report on phosphate glasses [28], no significant amounts of Nb dissolve in the Be-silicate glass melt.

3.3. Thermal properties

The thermal properties of all xNNaBe(Li) glasses were determined from DTA curves, which clearly show the glass transition temperature T_g and exothermic processes. The glass transition $T_{g,onset}$, the first exothermic process onset $T_{exo1,onset}$ and peak position $T_{exo,peak}$ temperatures as well as glass stabilities S_1, S_2 for all glasses are listed in Table 3. The glass stability is an often-used indicator describing the resistance of glass to crystallization during heating. It is typically expressed by the difference between the first crystallization onset value and the glass transition temperature $S_1 = T_{exo1,\ onset} - T_{g,onset}$ [46], or the first exothermic peak position and glass transition temperature $S_2 = T_{exo1,\ peak} - T_{g,onset}$ [47].

Table 3 Thermal properties of glasses xN(Li)NaBe: $T_{g,\ onset}$, $T_{exo,\ onset}$, $T_{exo,\ peak}$, S_1, S_2; obtained from DTA spectra. For comparison, the thermal properties values are included for glasses $35M_2O$-$65SiO_2$ and $35M_2O$–5BeO–$60SiO_2$ from ref. [5].

ID	$T_{g,\ onset}$ (°C) +/- 2%	$T_{exo1,onset}$ (°C) +/- 2%	$T_{exo1,peak}$ (°C) +/- 2%	S_1 (°C) +/- 4%	S_2 (°C) +/- 4%
0Na	484	746	788	262	304
0NaBe	507	736	786	229	279
1NNaBe	497	835	852	338	355
2NNaBe	498	830	856	332	358

3NNaBe	508	892	917	384	409
4NNaBe	517	895	909	375	392
5NNaBe	516	930	966	414	450
0LiNa	431	689	712	258	281
0LiNaBe	456	663	726	207	270
1NLiNaBe	447	743	793	296	346
2NLiNaBe	446	-	789	-	343
3NLiNaBe	458	-	821	-	363
4NLiNaBe	470	832	854	362	384
5NLiNaBe	473	847	848	374	375

Firstly, let us discuss the glass transition T_g results for the xN(Li)NaBe glass series. The T_g for 1NNaBe and 2NNaBe (~497 ^oC) as well as for 1NLiNaBe and 2NLiNaBe (~447 ^oC) glasses have similar values, while it increases with further addition of Si_3N_4. The observed difference between 1NNaBe and 5NNaBe glass is ~20 ^oC and between 1NLiNaBe and 5NLiNaBe glass it is ~26^oC. Figure 6 presents the glass transition temperature as a function of the summed Be+Si+N levels for all studied glasses. This kind of property (T_g) versus composition (Be+Si+N) presentation takes into account all elements which contribute to the cross-linking of the glass network. Specifically, BeO acting as intermediate glass-forming oxides will participate in the glass network with $[BeO_{4/2}]^{2-}$ tetrahedra, which are inserted in the network and strongly cross-link the silicate units through Si-O-Be bridges, thus causing the increase in T_g [5]. When nitrogen is chemically bonded to the silicon in the glass network as it substitutes for oxygen, a stiffer, more cross-linked network ensues due to its three-fold coordination. As observed in Fig. 6, an almost linear increase of T_g with Be+Si+N content is demonstrated for both glass series. However, since the Be content is almost constants for all glasses, the observed increase can mostly be attributed to different N and Si levels (both Si and N increase as Si_3N_4 is added to each glass series). It is also apparent that T_g results for glasses xNLiNaBe, in which 9 mol% of Na_2O was replaced by Li_2O, exhibit lower glass transition temperatures than the corresponding glasses containing sodium only (xNNaBe). The same trend was observed for glasses prepared in air [5]. Interestingly, the glass 0BNL has even a lower T_g than for the binary $34Li_2O$-$66SiO_2$ glass (456 °C, [48]), despite the 1 mol% higher modifier content in our 0NLBe glass. The much lower crosslinking capability of lithium ions compared to sodium ions

in silicate glasses seems to be compensated by a mixed modifier effect. Thus, the T_g decreases even more for the mixed compared to the pure Li-glass.

Results obtained for the xN(Li)NaBe glass series were compared with N-free (0NaBe and 0LiNaBe) and also Be-free (0Na and 0LiNa) glasses [5]. First, we discuss the changes in thermal behavior observed as a result of Be and N doping for the xNLiNaBe glass series. The increase of T_g observed as a result of doping 0LiNa glass with BeO is ~16 ^oC or ~25 ^oC, found for 1NLiNaBe and 0NaBeLi glasses, respectively. The higher value for 0NaBeLi can be attributed to additional Al^{3+} (~2.5 at%). However, the T_g of 4NLiNaBe and 5NLiNaBe glasses is higher even than that of 0LiNaBe; their T_g values increase by ~40 ^oC when compared to the undoped glass 0LiNa. Based on these results for the xNLiNaBe glass series, it can be assumed that addition of ~1.6 %at of Be increases the T_g by ~16 ^oC, and further addition of 2 at% of Al increases T_g by another ~9 ^oC. A similar increase is observed when doping the Al-free glasses with ~2 at% of N. The highest increase in T_g (up to ~26 ^oC), is seen for the incorporation of ~3.4 at% of N. A similar behavior is also observed for the xNNaBe glass series. Interestingly, a higher slope is observed in Fig. 6 for glasses xNLiNaBe than glasses xNNaBe. This result may be due to the higher content of N, which was detected by SEM-EDS for glasses 3NLiNaBe, 4NLiNaBe and 5NLiNaBe.

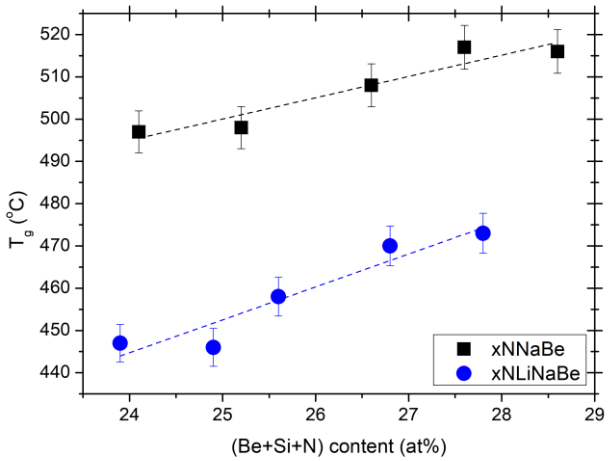

Figure 6 The dependence on the analyzed Be+Si+N content for $T_{g,\ onset}$ values for glasses xNNaBe and xNLiNaBe studied in this work. Lines between data points show trends of T_g - and are given as guides for the eyes only.

Table 3 depicts also the thermal glass stability (S_1 and S_2) for all glasses xN(Li)NaBe. It is evident that all xNNaBe and xNLiNaBe glasses show higher values of *S* than their reference glasses [5]. Moreover, glasses doped with lithium (xNLiNaBe) show in general lower values of thermal stability than the corresponding glasses containing only sodium (xNNaBe), similarly to T_g values. In our previous work [5], we have shown that beryllium addition decreases the glass stability in both Na-Al-Si-O and Li-Na-Al-Si-O glass systems in approximately a monotonic way. Contrary to Be doping, this work shows that an increase in the contents of both N and Si increases glass stability as observed for phosphate glasses [28]. Based on this knowledge we can assume that Al which is present in 0(Li)Na and 0(Li)NaBe glasses has an analogous effect as Be addition on the *S* value. The strongest influence of N incorporation into the silicate network is observed for glasses 5NNaBe and 4NLiNaBe, and this is in accordance with the estimated N content (see Table1).

Conclusions

Two different glass series with nominal composition close to $35M_2O$-5BeO-(60-x)SiO_2-xSi_3N_4, where M is Na or Na+Li and SiO_2 was substituted by up to 5 mol% Si_3N_4, were prepared in this work. All materials were found to be X-ray amorphous while the topography and composition of their cross-sections were homogenous and reproducible. All glasses were found to contain N, the content of which is highest for glasses doped with 5 mol% of Si_3N_4.

The results of Raman spectroscopy showed a high degree of spectral overlap between the studied glasses. Both glass series have silicate networks made up entirely of Q^3 and Q^2 silicate units, with higher content of Q^2 groups than in the analogous N- and Be-free silicate glasses. This difference can be attributed to the incorporation of $[BeO_{4/2}]^{2-}$ tetrahedra. A slight decrease in the Q^2 fraction is observed with Si_3N_4 addition, since this increases the network former to network modifier ratio. For the glass 5NLiNaBe, with the highest confirmed nitrogen content, the Q^2 signature is still high, but at the same time there is evidence for the formation of Q^4 units; thus, confirming the higher degree of network polymerization upon Si_3N_4 addition. Since three-fold bonded nitrogen substitutes for two-fold coordinated bridging oxygen atoms, a transformation of Q^n oxide species into Q^{n+1} oxy-nitride species is expected. In the case of 5NLiNaBe, disproportionation of Q^3 groups into Q^4 and Q^2 units was found to occur.

An increase in glass transition temperature is found for all (Li)-Na-Si-O glasses after doping with beryllium and incorporation of silicon and nitrogen into the silicate network. An increase in T_g (up to ~26 ^oC for Li-Na-Be-Si-O-N glass series) is observed as a result of Si and N incorporation. The incorporation of N also increases significantly the thermal stability of glasses.

Acknowledgements

SA, BJ and NAW acknowledge the financial support from the Crafoord Foundation (Grant No: 20160900). SA also acknowledges support from the Vinnova (Grant No. 2015-04809). DM thanks the Knowledge Foundation (Grant No. 68110029) for financing her stay at Linnæus University. EIK acknowledges the project “National Infrastructure in Nanotechnology, Advanced Materials and Micro - / Nanoelectronics” (MIS 5002772) which is implemented under the Action “Reinforcement of the Research and Innovation Infrastructure”, funded by the Operational Programme "Competitiveness, Entrepreneurship and Innovation" (NSRF 2014-2020) and co-financed by Greece and the European Union (European Regional Development Fund).

References

[1] V. Dimitrov, T. Komatsu, An interpretation of optical properties of oxides and oxide glasses in terms of the electronic ion polarizability and average single bond strength, Journal of the University of Chemical Technology and Metallurgy, 45 (2010) 219-250.

[2] S. Sen, P. Yu, Observation of a stuffed unmodified network in beryllium silicate glasses with multinuclear NMR spectroscopy, Physical Review B, 72 (2005) 132203. 10.1103/PhysRevB.72.132203

[3] E.I. Kamitsos, J.A. Kapoutsis, H. Jain, C.H. Hsieh, Vibrational study of the role of trivalent ions in sodium trisilicate glass, Journal of Non-Crystalline Solids, 171 (1994) 31-45. 10.1016/0022-3093(94)90030-2

[4] V.P. Klyuev, B.Z. Pevzner, Thermal expansion and transition temperature of glasses in the systems BeO-Al2O3-B2O3 and MgO-Al2O3-B2O3, Journal of Non-Crystalline Solids, 353 (2007) 2008-2013. 10.1016/j.jnoncrysol.2007.01.065

[5] N.A. Wójcik, S. Ali, D. Möncke, N.S. Tagiara, E.I. Kamitsos, H. Segawa, M. Eriksson, B. Jonson, The influence of Be addition on the structure and thermal propertiesof alkali-silicate glasses, Journal of Non-Crystalline Solids, 521 (2019) 119532 (1-10). 10.1016/j.jnoncrysol.2019.119532

[6] E. Morin, J. Wu, J. Stebbins, Modifier cation (Ba, Ca, La, Y) field strength effects on aluminum and boron coordination in aluminoborosilicate glasses: the roles of fictive temperature and boron content, Applied Physics A, 116 (2014) 479-490. 10.1007/s00339-014-8369-4

[7] C. Le Losq, D.R. Neuville, P. Florian, G.S. Henderson, D. Massiot, The role of Al3+ on rheology and structural changes in sodium silicate and aluminosilicate glasses and melts, Geochimica et Cosmochimica Acta, 126 (2014) 495-517. https://doi.org/10.1016/j.gca.2013.11.010

[8] L.M. Thompson, J.F. Stebbins, Non-stoichiometric non-bridging oxygens and five-coordinated aluminum in alkaline earth aluminosilicate glasses: Effect of modifier cation size, Journal of Non-Crystalline Solids, 358 (2012) 1783-1789. https://doi.org/10.1016/j.jnoncrysol.2012.05.022
[9] C.F. Lai, A. Silverman, Beryllium glass, Journal of the American Ceramic Society, 11 (1928) 535-541. DOI 10.1111/j.1151-2916.1928.tb17038.x
[10] C.F. Lai, A. Silverman, Beryllium glass, II Potassium-beryllium series, Journal of the American Ceramic Society, 13 (1930) 393-398. DOI 10.1111/j.1151-2916.1930.tb16289.x
[11] E.F. Riebling, D.A. Duke, BeO·Al2O3·SiO2 system: Structural relationships of crystalline, glassy, and molten beryl, Journal of Materials Science, 2 (1967) 33-39. 10.1007/bf00550050
[12] A.G. Clare, A.C. Wright, R.N. Sinclair, A comparison of the structural role of Na+ network modifying cations in sodium silicate and sodium fluoroberyllate glasses, Journal of Non-Crystalline Solids, 213 (1997) 321-324. Doi 10.1016/S0022-3093(97)00015-X
[13] W. Vogel, Glass Chemistry, 2 ed., Springer-Verlag, 1992
[14] I.S. Zhidkov, A.F. Zatsepin, S.O. Cholakh, Y.A. Kuznetsova, Optical properties and structure of beryllium lead silicate glasses, in, AIP Conference Proceedings, 2014, pp. 185-191. 10.1063/1.4900476
[15] K.-U. Hess, D.B. Dingwell, S.L. Webb, The influence of alkaline-earth oxides (BeO, MgO, CaO, SrO, BaO) on the viscosity of a haplogranitic melt; systematics of non-Arrhenian behavior, European Journal of Mineralogy, 8 (1996) 371-381.
[16] S. Ali, B. Jonson, T. Rouxel, Glasses in the Ba-Si-O-N System, Journal of the American Ceramic Society, 94 (2011) 2912-2917. 10.1111/j.1551-2916.2011.04718.x
[17] A. Sharafat, B. Forslund, J. Grins, S. Esmaeilzadeh, Formation and properties of nitrogen-rich strontium silicon oxynitride glasses, Journal of Materials Science, 44 (2008) 664. 10.1007/s10853-008-3058-3
[18] A. Sharafat, J. Grins, S. Esmaeilzadeh, Glass-forming region in the Ca–Si–O–N system using CaH2 as Ca source, Journal of the European Ceramic Society, 28 (2008) 2659-2664. 10.1016/j.jeurceramsoc.2008.04.017
[19] A. Sharafat, B. Forslund, J. Grins, S. Esmaeilzadeh, Formation and properties of nitrogen-rich strontium silicon oxynitride glasses, J. Mater. Sci., 44 (2009) 664-670. DOI 10.1007/s10853-008-3058-3
[20] A. Sharafat, J. Grins, S. Esmaeilzadeh, Properties of high nitrogen content mixed alkali earth oxynitride glasses (AExCa1−x)1.2(1)SiO1.9(1)N0.86(6), AE=Mg, Sr, Ba, Journal of Non-Crystalline Solids, 355 (2009) 1259-1263. https://doi.org/10.1016/j.jnoncrysol.2009.04.036
[21] A. Sharafat, J. Grins, S. Esmaeilzadeh, Hardness and refractive index of Ca–Si–O–N glasses, Journal of Non-Crystalline Solids, 355 (2009) 301-304. https://doi.org/10.1016/j.jnoncrysol.2008.11.019
[22] S. Ali, B. Jonson, Compositional effects on the properties of high nitrogen content alkaline-earth silicon oxynitride glasses, AE=Mg, Ca, Sr, Ba, Journal of the European Ceramic Society, 31 (2011) 611-618. https://doi.org/10.1016/j.jeurceramsoc.2010.11.005
[23] S. Ali, B. Jonson, Preparation of oxynitride glasses from woody biofuel ashes, Journal of Non-Crystalline Solids, 356 (2010) 2774-2777. 10.1016/j.jnoncrysol.2010.09.071
[24] T. Das, Oxynitride glasses - An overview, B Mater Sci, 23 (2000) 499-507. Doi 10.1007/Bf02903891
[25] S. Sakka, Structure, Properties and Application of Oxynitride Glasses, Journal of Non-Crystalline Solids, 181 (1995) 215-224. Doi 10.1016/S0022-3093(94)00514-1
[26] N. Mascaraque, J.L.G. Fierro, A. Durán, F. Muñoz, An interpretation for the increase of ionic conductivity by nitrogen incorporation in LiPON oxynitride glasses, Solid State Ionics, 233 (2013) 73-79. 10.1016/j.ssi.2012.12.017
[27] M.R. Reidmeyer, D.E. Day, R.K. Brow, Phosphorus Oxynitride Glasses of Variable Sodium Content, Journal of Non-Crystalline Solids, 177 (1994) 208-215. Doi 10.1016/0022-3093(94)90532-0
[28] N. Wojcik, D. Möncke, ... Influence of synthesis conditions on glass formation, structure and thermal properties in the Na2O-CaO-P2O5 system doped with Si3N4 and Mg, Journal of Non-Crystalline Solids, 494 (2018) 66 - 77. https://doi.org/10.1016/j.jnoncrysol.2018.04.055

[29] N.A. Wójcik, B. Jonson, R.J. Barczyński, P. Kupracz, D. Möncke, S. Ali, Electrical properties of Na2O-CaO-P2O5 glasses doped with SiO2 and Si3N4, Solid State Ionics, 325 (2018) 157-162. https://doi.org/10.1016/j.ssi.2018.08.011
[30] M.A. Carrillo Solano, M. Dussauze, P. Vinatier, L. Croguennec, E.I. Kamitsos, R. Hausbrand, J. W., Phosphate structure and lithium environments in lithium-phosphorus oxynitride amorphous thin films, Ionics, 22 (2016) 471-481.
[31] M. Dussauze, E.I. Kamitsos, P. Johansson, A. Matic, C.P. Varsamis, D. Cavagnat, P. Vinatier, H. Y., Lithium ion conducting boron-oxynitride amorphous thin films: Synthesis and molecular structure by infrared spectroscopy and density functional theory modeling, J. Phys. Chem. C, 117 (2013) 7202-7213.
[32] S. Ali, B. Jonson, M.J. Pomeroy, S. Hampshire, Issues associated with the development of transparent oxynitride glasses, Ceramics International, 41 (2015) 3345-3354. https://doi.org/10.1016/j.ceramint.2014.11.030
[33] I. Konidakis, C.P.E. Varsamis, E.I. Kamitsos, Effect of synthesis method on the structure and properties of AgPO3-based glasses, Journal of Non-Crystalline Solids, 357 (2011) 2684-2689. https://doi.org/10.1016/j.jnoncrysol.2011.03.013
[34] D. Palles, I. Konidakis, C.P.E. Varsamis, E.I. Kamitsos, Vibrational spectroscopic and bond valence study of structure and bonding in Al2O3-containing AgI-AgPO3 glasses, RSC Advances, 6 (2016) 16697-16710. https://doi.org/10.1039/C6RA00162A
[35] N.S. Tagiara, D. Palles, E.D. Simandiras, V. Psycharis, A. Kyritsis, E.I. Kamitsos, Synthesis, thermal and structural properties of pure TeO2 glass and zinc-tellurite glasses, Journal of Non-Crystalline Solids, 457 (2017) 116-125. https://doi.org/10.1016/j.jnoncrysol.2016.11.033
[36] S. BAIK, R. RAJ, Suppression of Frothing by Silicon Addition During Oxynitride Glass Synthesis, Journal of the American Ceramic Society, 68 (1985) C - 168-C - 170. doi:10.1111/j.1151-2916.1985.tb10161.x
[37] G.X. Wang, G.Q. Lu, B. Pei, A.B. Yu, Oxidation mechanism of Si3N4-bonded SiC ceramics by CO, CO2 and steam, Journal of Materials Science, 33 (1998) 1309-1317. 10.1023/a:1004354415867
[38] N.A. Wójcik, B. Jonson, D. Möncke, D. Palles, E.I. Kamitsos, E. Ghassemali, S. Seifeddine, M. Eriksson, S. Ali, Influence of synthesis conditions on glass formation, structure and thermal properties in the Na2O-CaO-P2O5 system doped with Si3N4 and Mg, Journal of Non-Crystalline Solids, 494 (2018) 66. 10.1016/j.jnoncrysol.2018.04.055
[39] G. Panczer, D. De Ligny, C. Mendoza, M. Gaft, A.M. Seydoux-Guillaume, X. Wang, Raman and fluorescence, in: European Mineralogical Union Notes in Mineralogy, 2012, pp. 61-82. 10.1180/EMU-notes.12.2
[40] T. Furukawa, K.E. Fox, W.B. White, Raman-spectroscopic investigation of the structure of silicate-glasses. 3. Raman intensities and structural units in sodium-silicate glasses, Journal of Chemical Physics, 75 (1981) 3226-3237. 10.1063/1.442472
[41] P. McMillan, Structural studies of silicate glasses and melts-applications and limitations of Raman spectroscopy, American Mineralogist, 69 (1984) 622-644.
[42] E. Stavrou, D. Palles, E.I. Kamitsos, A. Lipovskii, D. Tagantsev, Y. Svirko, S. Honkanen, Vibrational study of thermally ion-exchanged sodium aluminoborosilicate glasses, Journal of Non-Crystalline Solids, 401 (2014) 232-236. http://dx.doi.org/10.1016/j.jnoncrysol.2013.12.017
[43] M. Deng, G. Zhang, Y. Zeng, X. Pei, R. Huang, J. Lin, Simple process for synthesis of layered sodium silicates using rice husk ash as silica source, Journal of Alloys and Compounds, 683 (2016) 412-417. https://doi.org/10.1016/j.jallcom.2016.05.115
[44] H. Krüger, V. Kahlenberg, R. Kaindl, Structural studies on Na6Si8O19—a monophyllosilicate with a new type of layered silicate anion, Solid State Sciences, 7 (2005) 1390-1396. https://doi.org/10.1016/j.solidstatesciences.2005.08.002
[45] D. Möncke, R. Ehrt, D. Palles, I. Efthimiopoulos, E.I. Kamitsos, M. Johannes, A multi technique study of a new lithium disilicate glass-ceramic spray-coated on ZrO2 substrate for dental restoration, Biomedical Glasses, 3 (2017) 41-55. https://doi.org/10.1515/bglass-2017-0004

631 [46] A.R. Boccaccini, D.S. Brauer, L. Hupa, Bioactive Glasses: Fundamentals, Technology and
632 Applications, Royal Society of Chemistry, 2016
633 [47] V. Simon, D. Muresan, A. Takacs, M. Neumann, S. Simon, Local order changes induced in calcium–
634 sodium–phosphate glasses by transition metals, Solid State Ionics, 178 (2007) 221-225.
635 10.1016/j.ssi.2006.12.011
636 [48] T. Seuthe, M. Grehn, A. Mermillod-Blondin, H.J. Eichler, J. Bonse, M. Eberstein, Structural
637 modifications of binary lithium silicate glasses upon femtosecond laser pulse irradiation probed by
638 micro-Raman spectroscopy, Opt. Mater. Express, 3 (2013) 755-764. 10.1364/OME.3.000755

639